Dispersion affecting the VLTI and 10 micron interferometry using MIDI

Jeffrey Meisner and Rudolf Le Poole

Leiden Observatory, P.O. Box 9513, 2300RA Leiden, The Netherlands

ABSTRACT

A wideband interferometer is sensitive to the effects of longitudinal dispersion which affect the interfering light beams unequally. At shorter wavelengths the major effect of dispersion is from dry air itself, while at mid infrared wavelengths the effect of water vapor is dominant. MIDI, the future 10 micron instrument of the VLTI, will experience significant effects from the imbalances in the water vapor content affecting the paths of the two interfering beams. This imbalance will include terms due to the unbalanced air paths in the delay line, random atmospheric humidity fluctuations in the lines-of-sight to the star, and random humidity variations inside of the VLTI delay line tunnels.

Large amounts of dispersion, if not monitored, can reduce the accuracy of measured visibility amplitudes. Measurements of the visibility phase as a function of wavelength will be highly sensitive to dispersion. This will then become a source of noise in results dependent on the phase of interference, such as imaging of non-symmetric objects, or detection of faint companions. In addition to dispersion over the 7 - 14 micron region detected by MIDI, observations using phase tracking with detection in the near IR, could be catastrophically affected by differential phase delays between the 2 micron and 10 micron bands.

Dispersion measurements from VINCI observing in the K band, both due to dry air and to water vapor, are presented. Combining VINCI results with published data from millimeter wave measurements leads us to expect atmospheric differential water vapor fluctuations to exceed 1 $mole/m^2$ rms over typical baselines. Specific effects from such a level of unmonitored dispersion variations are presented, which demand corrective action. Various solutions to monitor water vapor dispersion in realtime are considered.

Keywords: Stellar interferometry, dispersion, water vapor, atmosphere, phase, group delay, infrared

1. INTRODUCTION

In the past most stellar interferometry in the $10\mu m$ band has been performed using *heterodyne* interferometry, which is extremely narrow-band and thus not sensitive to dispersion. New $10\mu m$ interferometric instruments are planned at the VLTI, the Keck interferometer, and LBT. With direct detection $10\mu m$ interferometry, worries concerning the dispersion due to water vapor have come to the fore. Scientists involved in the construction of MIDI, the $10\mu m$ instrument soon to be installed at the VLTI, decided that this issue required more intensive research, which was therefore begun.

Three aspects of the problem were identified which this paper attempts to answer:
1) What is the material dispersion (index of refraction as a function of optical frequency) of water vapor in the $10\mu m$ band?
2) How would the actual amounts of water vapor in the atmosphere and in the internal light paths of VLTI affect interferometric observations at $10\mu m$?
3) What corrections (in hardware or software) might be employed to reduce any deleterious effects due to water vapor dispersion?

This paper sums up the current state of our research in this regard, and presents a number of important conclusions.

email: meisner@strw.leidenuniv.nl

Dispersion can affect a stellar interferometer in *hardware*, meaning that the measured fringe visibility is compromised due to an uncorrectable phase variation among wavelengths interfered upon a single detector element. Secondly, dispersion can effect the results of processing interferometric data in the case that visibility estimators are employed which are sensitive to, but not adjusted for, the effect of phase variations due to dispersion.

Dispersive effects at the *hardware* level, clearly lead to a loss of information (i.e. SNR reduction) which cannot be recovered in the data processing. This is a serious concern at visible wavelengths (particularly toward the blue) where the dispersion of air is very large, and when one attempts to detect light over a very wide bandwidth simultaneously without optical dispersion compensation.[1,2] However losses at the detection stage can be reduced by using spectrally-dispersed detection in which every detector element sees light only of a narrow-bandwidth. Furthermore, in the infrared, at which all of the newer interferometers are primarily intended, we find a lesser magnitude of dispersion, so that pre-detection (optical) correction of dispersion is not an absolute necessity *except* in the case of a nulling interferometer. Although in other cases dispersion will not necessarily demand hardware correction, it *will* affect the eventual results, at least using some forms of data reduction. We shall therefore attempt to understand, qualitatively and quantitatively, the scope of this problem and various remedies. We will limit our investigation to the infrared regime, with particular emphasis on wideband interferometry at $10\mu m$, as will soon be undertaken at the VLTI using MIDI.

2. MATHEMATICAL DESCRIPTION OF DISPERSION AND TERMINOLOGY

Let us briefly review the fundamental mathematical description of dispersion and the use of terms employed in this paper. *Dispersion* refers to any phase function which (in the frequency range of consideration) departs from an achromatic delay. An achromatic delay implies a linear relation between phase ϕ and frequency ν *with no phase offset at zero frequency:*

$$\phi = 2\pi\tau\,\nu$$

Dispersion occurs for any other phase function *including* a constant phase. For lack of better terminology, we shall loosely use the word "dispersion" to apply to such a phase relationship itself, to *material dispersion* such as passage through glass, and to *lumped dispersion* such as the phase shift at a reflection.

A fundamental concept is the *phase delay* given by

$$\tau_p = \frac{1}{2\pi}\,\frac{\phi}{\nu} \quad .$$

If all frequencies have the same phase delay then there is no dispersion present. Although a less fundamental concept than phase delay, the group delay is also of great importance in many contexts. It is defined as

$$\tau_g = \frac{1}{2\pi}\,\frac{d\phi}{d\nu} \quad .$$

Under conditions of no dispersion, the group delay is constant at all frequencies (in the range of consideration) *and* is equal to the phase delay (which is also constant). Unlike the phase delay, the group delay suffers no mathematical ambiguity due to arbitrary 2π offsets in the description of the phase function. However the group delay alone is insufficient to specify a phase function.

First order dispersion occurs whenever the group delay is constant (in the frequency range considered) but is *not* identical to the phase delay. Figure 1A shows a fringe (or wave packet) which has been affected by first order dispersion. The envelope of the fringe is unchanged from what it was before suffering dispersion, but the relative position of the group delay (given by the position of the peak of the envelope) and the phase delay at the center frequency (given by the peaks of the signal itself) are offset. The *group delay offset phase* Φ_{GD} (often simply referred to as the "dispersion phase") is defined as:

$$\Phi_{GD}(\nu) = 2\pi\,\nu\,(\tau_g(\nu) - \tau_p(\nu))$$

In first order dispersion, Φ_{GD} is constant at all frequencies.

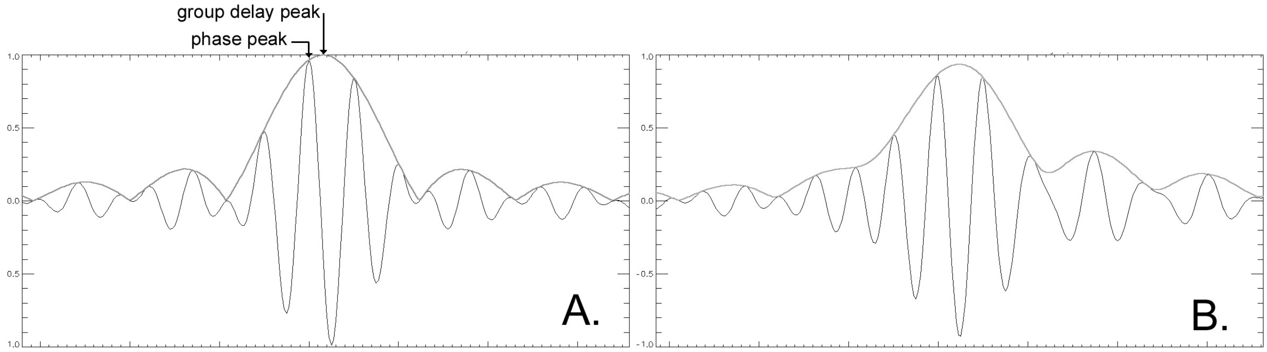

Figure 1. **A:** Fringe affected by first order dispersion only: Φ_{GD}=2 radians. **B:** A highly dispersed fringe in which higher order dispersion is apparent in the envelope asymmetry and "chirping."

Higher order dispersion affecting the fringe of Fig. 1A is depicted in Fig. 1B. With higher order dispersion, the fringe envelope is generally widened, is no longer symmetric, and the frequency content can change along the fringe ("chirping"). Neither the phase, the phase delay, the group delay, nor Φ_{GD} is constant with respect to frequency.

In stellar interferometry, a well defined point of "zero delay" generally does not exist or cannot be observed. It is important to note that the addition of an arbitrary delay to a transfer function or wave packet does not alter the dispersion as we have defined it.*

In this paper we will most often be referring to *material dispersion*, that is, the phase of the transfer function occurring due to passage of a light wave through a length L of a transparent material whose index of refraction is given by n. That phase, and the associated phase delay, are then given by:

$$\phi = \frac{2\pi\,\nu\,L\,n(\nu)}{c} \qquad \tau_p = \frac{L\,n(\nu)}{c} \quad .$$

In order to concentrate on the effect of the material itself, let us change the "zero point" of our delay measurements, removing the vacuum delay L/c from consideration.

$$\phi' = \frac{2\pi\,\nu\,L}{c}\,(n(\nu)-1) \qquad \tau_p' = \frac{L}{c}\,(n(\nu)-1)$$

Having subtracted unity from the index of refraction, we are left with a refractivity $n-1$ which, for transparent gasses at normal pressures, is generally much less than one. That allows us to bypass the Clausius-Mossotti relationship, and simply consider the refractivity of a gas mixture as the sum of the refractivities of its components. It also therefore allows us to consider the refractivity as a constant for the substance multiplied by the density of the gas. Finally, it allows us to consider the phase shift or the phase delay to be solely dependent on the net *column density* of the gas through which it has passed. For a gas whose refractivity is $n-1$ at a molar density ρ, we then define the *normalized refractivity* $\hat{n}$ as:

$$\hat{n}(\nu) = \frac{n(\nu)-1}{\rho\,c}$$

We express $\hat{n}$ in units of femtoseconds delay per $mole/m^2$ column density. Using the normalized refractivity allows us to concentrate on the optical properties of a gas without specifying the temperature, pressure, or its concentration in a mixture. Then we can always determine the phase delay in travel through a gas as equal to the vacuum delay L/c due to the *distance* travelled (which is dispersion free), plus the extra delay due to the gas given by $\hat{n}$ times the column density D of the gas in its path. Here are some useful conversions:

*Extending the definitions put forward, one could properly identify achromatic delays as "zero-order dispersion." Also note that some authors do not include first order dispersion within their definition of dispersion.

- Gas at 1mm Hg at 0° C: $D = L \cdot .0587\, mole/m^3$
- Gas at STP (760mm Hg, 0° C): $D = L \cdot 44.6\, mole/m^3$
- 1mm precipitable water vapor: $D = 55.5\, mole/m^2$
- Entire atmosphere (1 airmass): $D \approx 350,000\, mole/m^2$

Now we can, for instance, multiply the normalized refractive index of air by the density of air at atmospheric pressure, to obtain the additional delay (relative to propagation in a vacuum) per meter.

$$\tau_p = \hat{n} \cdot D = 21.5\, fs/(mole/m^2) \cdot (44.6\, mole/m^3 \cdot L) = 959 fs/m \cdot L$$

Having defined $\hat{n}$, we can finally introduce the normalized "dispersion constant" K, defined as:

$$K = 2\pi\, \nu^2 \frac{d\hat{n}}{d\nu} \quad .$$

The dispersion constant for a substance at an optical frequency ν is a measure of the qualitative effect of dispersion due to a quantity of that substance which is comparable across wide frequency ranges. It directly supplies the magnitude of first order dispersion Φ_{GD} due to a column density D of that substance:

$$\Phi_{GD} = K \cdot D \quad .$$

If only first order dispersion is considered to be present, then the dispersion constant specifies the resulting phase shift (in radians) across a given *fractional* bandwidth $B = \Delta\nu/\nu_0$:

$$\Delta\phi = B \cdot \Phi_{GD} = K \cdot D \cdot B \quad .$$

3. INDEX OF REFRACTION OF AIR AND WATER VAPOR IN THE IR

In addition to the *fixed* instrumental dispersion due to optical components (lenses, windows, beamsplitters, etc.) dispersion affecting optical stellar interferometry is the result of passage through air having various humidities. There have been numerous measurements of the refractivity of air (with humidity considered) in the visible and at near IR wavelengths used for range-finding equipment, but actual measurements farther in the infrared are scarce. One area of follow-up work involved in the present study includes experimental measurement of these quantities. For now, we present our best knowledge of these values based on a combination of experiment and analysis.

3.1. Dry Air

Let us first consider "dry air," that is, air in which any water vapor has been removed. There is relatively little variation among the constituents of dry air which will affect its refractive index, particularly over short distance scales (with a possible exception in the case of nearby machinery generating large amounts of CO_2, O_3, or NO_x). Thus it is probably realistic to model dry air as a single substance having a given refractivity proportional to its density.

Over the visible and infrared wavelength bands, the major constituents of air, N_2 and O_2, do not have strong transitions, thus the dispersion of dry air is almost totally due to UV lines. The result is a quite smooth variation of refractive index over infrared (and most visible) wavelengths. This relation has been approximated using various empirical formulae[3–5] which predict similar curves. In the upper left of Fig. 2, the formula of Ciddor[5] for the refractivity of dry air is shown in terms of normalized units (femtoseconds phase delay per column density in $mole/m^2$). It can be seen that dry air has very little dispersion in the infrared. It should be pointed out, however, that while this formula appears to accurately predict the refractivity of dry air based on its major constituents, large effects due to CO_2 in certain regions have been overlooked. CO_2 transitions around $4\mu m$ and $15\mu m$ do contribute substantial additional dispersion at nearby frequencies in the L and M bands, and in particular at the long wavelength end of the N band. The (possibly variable) concentration of CO_2 at Paranal will need to be taken into account in order to accurately model the air in the delay lines. There may also be a small effect around $9.5\mu m$ due to any ambient ozone.

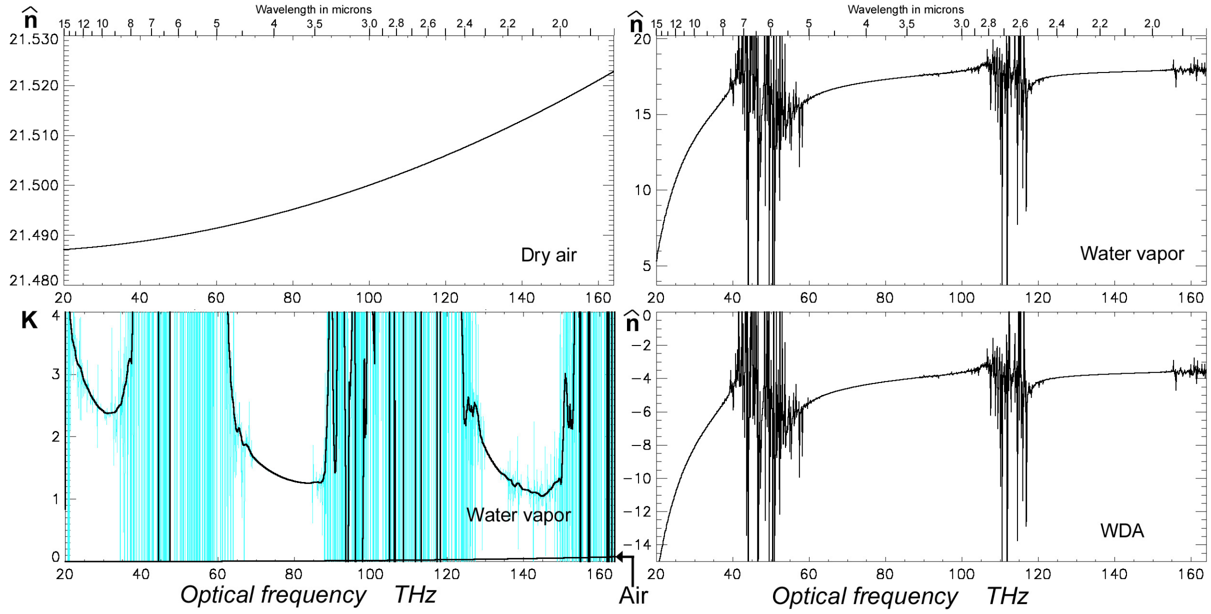

Figure 2. Normalized index of refraction $\hat{n}$ in units of fs/$(mole/m^2)$. Upper left: dry air; Upper right: water vapor; Lower right: "WDA" (see text for explanation). Lower left: the dispersion constant K of water vapor in radians/$(mole/m^2)$, with the smooth bold line plotting the median filtered value in the continuum regions. The tiny value of K for dry air is shown near the bottom for comparison.

3.2. Water Vapor

We will now examine the case of water vapor which typically composes .2 - 2% of the molar volume of air at ground level. While there have also been empirical formula proposed for the refractivity of water vapor,[4] it has recently become clear that these models have failed to account for the actual dispersion of water vapor in the infrared. We base the following results on a computation performed by Richard Mathar[6] using over 30,000 water vapor absorption lines in the infrared. Since this work was only intended to predict the dispersion, but not the overall magnitude of the refractivity of water vapor, we must add a constant term, presumably due to ultraviolet transitions which had been ignored, in order to agree with empirical measurements performed by Matsumoto.[7] At wavelengths longer than $7\mu m$ this result is in good agreement with an earlier analysis by Hill and Lawrence,[8] but Mathar claims validity at shorter wavelengths and indeed his results are consistent with dispersion observed at K band (see Fig. 4C and D).

The net result for the normalized refractivity of water vapor is shown in the top right of Fig. 2, in which one can appreciate the true slope of refractivity (dispersion) in regions not polluted by the presence of spectral features. We have computed the dispersion constant K implied by this refractivity in the lower left of the same figure. We can see that it has a similar order of magnitude in each of the IR windows, but with a modest increase toward longer wavelengths. In particular, we find that the dispersion constant is about twice as large in the N band compared to the K band. Thus when there is a water vapor imbalance which causes a group-delay offset phase Φ_{GD} of 1 radian in the middle of the K band, that will translate to 2 radians in the N band; this will result from a column density of about .8 $mole/m^2$.

3.3. "WDA"

In some instances, rather than talking about water vapor directly, it will be convenient to refer to a third quantity. If we hold the total pressure and the temperature constant, then any humidity added to the air reduces the amount of dry air by an equal molar volume. Thus we shall define a fictitious substance called "Water vapor Displacing Air" (WDA). A mole of WDA is defined as one mole of water vapor plus one *negative* mole of dry air. Consequently it has an index of refraction $\hat{n}_{wda}$ (which is negative at our wavelengths) given by $\hat{n}_{water} - \hat{n}_{air}$ as graphed in the lower right of Fig. 2. Employing the concept of WDA, we can view a quantity of air as consisting of an amount of dry air given solely by the ambient temperature and pressure *plus* a quantity of WDA representing the humidity. The net partial pressure from WDA is exactly zero. This contrivance essentially allows us to view these as two non-interacting substances existing in the same space.

Looking at the lower left graph of Fig. 2., we can see that in the infrared, dispersion due to WDA (essentially the same as for simple water vapor) is very much greater than that due to dry air. On the other hand, there is much more dry air present than WDA. Let us now look at two particular problems involving an infrared stellar interferometer, and see what the effects of dispersion will be due to these substances.

4. DISPERSION DUE TO AIR MIXTURES IN UNBALANCED DELAY LINE PATHS

An interferometer requires a delay line in order to equalize the total OPD travelled by the light from the star over two (or more) paths. The angle of the star from the "zero-OPD" position implies an imbalance in the light paths *in space*. However the delay lines and optical paths following the telescopes, in most interferometers (including the VLTI), occurs in air, not vacuum. As a result, there is a very substantial imbalance in the light paths reflecting the dispersion of that amount of air.

Because this optical travel occurs within the confines of the interferometer's infrastructure in a controlled environment, we will refer to this effect as "instrumental dispersion" and regard it as being non-random. In practice, that is an idealization: there will very likely be not only random temperature, but also humidity fluctuations in the air inside the interferometer's infrastructure, so the best we could really hope for is that the composition of that air can be accurately monitored. Even that has not been implemented in most interferometers. In the case of the VLTI, the air paths and delay line tunnels are open to the outside and normally get flushed with fresh air, so the best estimate of the composition of the delay line air, is that of the outside air at a slightly warmer temperature. Thus there will be a small (but potentially significant) unmonitored component of dispersion in the excess air paths, which will contribute to the random component of dispersion discussed in Sect. 5. However we would now like to concentrate on the large fixed component of dispersion due to this unbalanced propagation in air.

We consider the excess delay line path to consist mainly of dry air, as we have defined it, at the ambient atmospheric pressure. Additionally there is a small amount of WDA (water vapor) present. In the case of the VLTI, a relatively dry location, the water vapor accounts for only about .3% of the total air volume. This corresponds to the typical conditions of 15% relative humidity at 13^o C; at the location of a different interferometer, its abundance could be several times higher. Because of this proportion, the net dispersion due to dry air is enhanced by some 300 relative to that of water vapor. On the other hand, the material dispersion in the infrared due to 1 $mole/m^2$ of water vapor is much higher than for air. Let us see, then, what the net effect of these two constituents are at different wavelengths.

4.1. Dispersion Constant for Delay Line Air at Infrared Wavelengths

The relevant quantity, again, is the dispersion constant, which is plotted in Fig. 3. against optical frequency for three different air compositions. The middle graph corresponds to air with .3% water vapor, typical for Paranal. The upper curve is for air with 1% water vapor composition as might be experienced at an interferometer at a more humid location. The contribution to the dispersion due to dry air alone can be seen in the dashed curve at the bottom.

It can be seen that the overall dispersion per $mole/m^2$ of air path is somewhat smaller at N band that at K band due to the very small dispersion of dry air at long wavelengths. At K band most of the dispersion is due to dry air, with a rather small (but significant) contribution from water vapor. Not shown, is the visible region, where the dispersion constant due to dry air is yet 100 times higher, thoroughly overshadowing any effect due to humidity.

To interpret the quantity K shown in this plot, bear in mind that this gives the group delay offset phase Φ_{GD} in radians per $mole/m^2$ of excess air path, and that every meter of air path in the delay lines at Paranal has

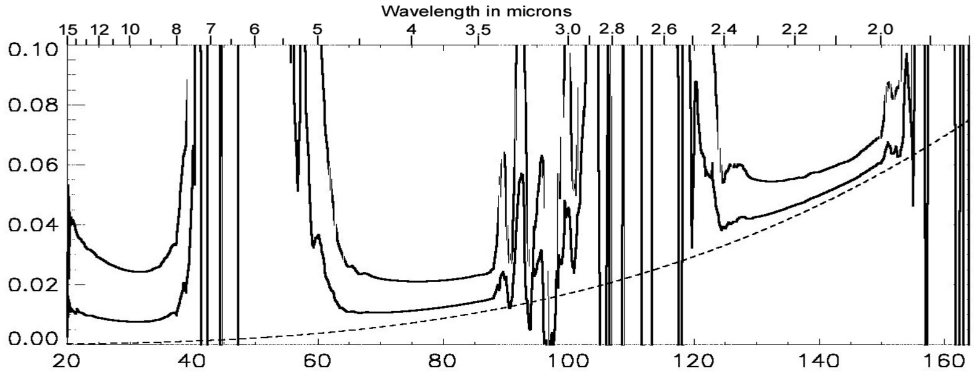

Figure 3. Dispersion constant K in radians per $(mole/m^2)$ versus optical frequency (THz) for air that might be present in an interferometer's delay lines. Bottom (dashed) plot shows the dispersion constant for dry air, middle plot is for air with .3% water vapor (typical for Paranal), and the top plot is for humid air with 1% water vapor content.

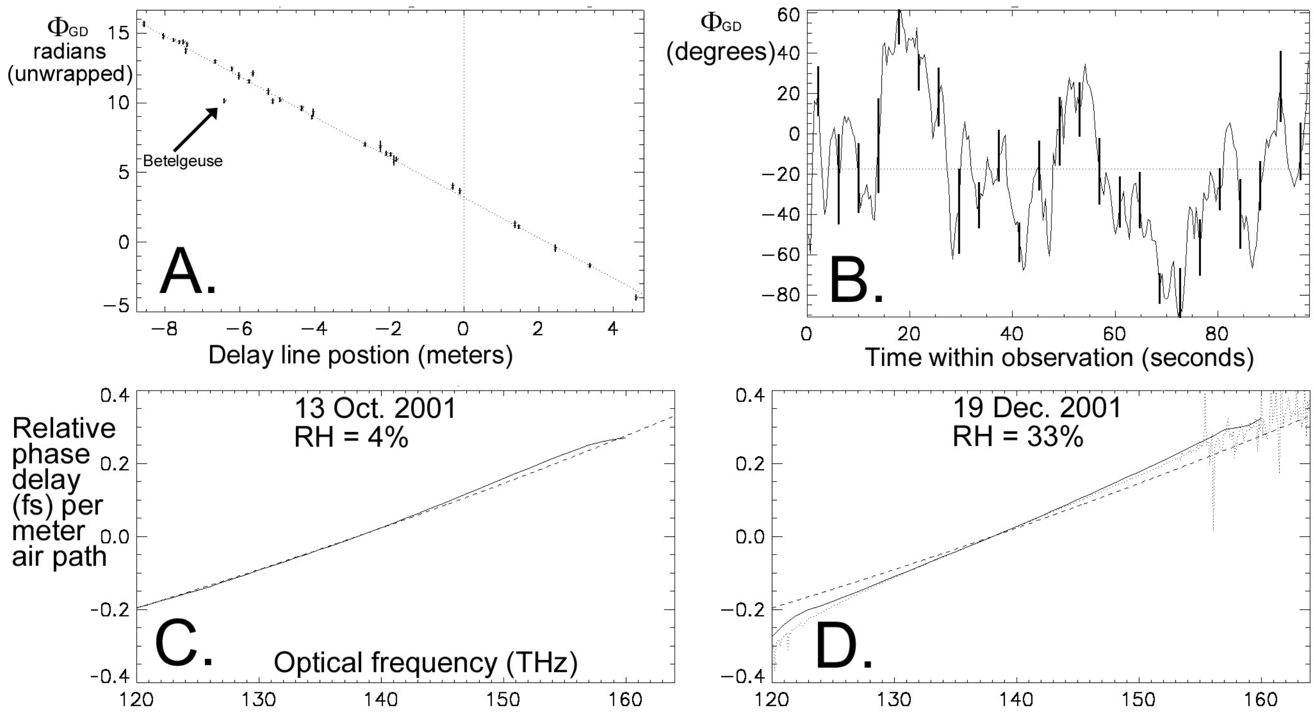

Figure 4.
A: Fit of first order dispersion versus differential air path using 35 VINCI observations on 13 Oct. 2001.
B: Observed time variation of Φ_{GD} *within* a VINCI observation of Sirius, with $\pm 1\sigma$ error bars plotted at regular intervals.
C: Phase delay vs. optical frequency, combining higher order dispersion with dispersion slope per meter air path shown in A. Dashed line is prediction for dry air at ambient pressure.
D: Same as C but for a very humid night. Predictions for dry air (dashed) and air with .007 water vapor content (dotted) are plotted.
Sidelight: Calibration of delay line air dispersion shown in A allows rough determination of source Φ_{GD}. Observation of Betelgeuse shows an offset from the calibration (expected to be π radians) due to its negative visibility in this observation performed beyond the first null.

approximately 31.5 $mole/m^2$ (depending on the temperature and barometric pressure) of moist air. Multiplying the dispersion constant at 138THz by this quantity, we obtain first order dispersion at a rate of 1.50 radians per meter.

4.2. Experimental Measurement of Delay Line Dispersion

Changes in Φ_{GD} as a function of delay line position, at approximately this rate, have been observed at PTI,[9] and more recently using data from VINCI,[10] the K band commissioning and alignment instrument for the VLTI. In Fig. 4A dispersion is plotted against differential air path for 35 observations performed by VINCI on various stars on 13 October, 2001. The observed phases have been "unwrapped" to fit a straight line, whose slope in this case was found to be 1.46 radians per meter at the mean effective optical frequency of 138 THz.

A similar procedure was used to examine the residual phase as a function of optical frequency for each observation after removing the component of first order dispersion, and at each frequency fitting a slope versus the delay line position of the 35 contributing observations. The net result, including the major effect of first order dispersion, is plotted over the detected bandwidth (120 - 160 THz) in Fig. 4C. Also plotted in a dashed line, is the theoretical dispersion due to dry air at a density of 31.2 $mole/m^3$, appropriate for the temperature and pressure that night. Note that the arbitrary zero point of the quantities plotted in Fig. 4C and D have all been adjusted to match at 138 THz.

4.3. Effect of Humidity

The data plotted in Fig. 4C was on a night of very low humidity, even by Paranal standards, where the proportion of water vapor in the air was about .09%. To directly observe the effect of water vapor in delay line dispersion, we identified a night of unusually high humidity (but when it was clear for observing) at Paranal and repeated the same exercise. On 19 December 2001 the relative humidity varied between about 25 and 40%, or an average atmospheric water vapor content of about .7%. The result, shown in Fig. 4D can be compared again to the prediction for dry air shown (dashed line) and one predicted for air with 33% humidity (dotted line). Our assumption is that the air in the VLTI light paths will reflect the humidity of the outside air which is allowed to freely flow through the tunnels.

5. ATMOSPHERIC DISPERSION AND OPD FLUCTUATIONS

We have seen that travel through many meters of excess air path in the delay lines (and other light paths) will incur a large amount of dispersion. Because that air path consists of over 99% dry air, we find it to be the dominant dispersive ingredient at near infrared wavelengths.

Now let us turn to the question of *random atmospheric* dispersion. Here the situation is reversed! Even though the line-of-sight to a star may pass through 1000 times as much dry air as water vapor, the *differential* dispersive effect of the water vapor is much greater, even at K band. Let us see why that is the case.

5.1. Dry Air and Water Vapor Inhomogeneities in the Atmosphere

Integrated density variations in the air through the path of the light through the atmosphere are caused by minor temperature differences in the air of that path. Any actual horizontal *pressure* differences in the air (except on large scales, that is, weather-related) will immediately cause an air flow from higher to lower pressure, balancing the pressure difference. Thus only small density variations remain due to small temperature inhomogeneities. This, of course, is the source of astronomical "seeing" as well as the overall OPD fluctuations encountered by a stellar interferometer. In the case of Paranal, over a typical baseline of 66 meters, we find (using VINCI) an rms OPD variation of about 30 femtoseconds (or 10 microns pathlength) on a good night. This corresponds to about 1.5 $mole/m^2$ of column density of air. The total air mass in the line-of-sight (towards zenith) is about 250,000 $mole/m^2$. Thus the random component is less than 10^{-5} of the total air column.

Water vapor in the atmospheric line-of-sight, however, is not constrained by the requirement that there be no static horizontal pressure variations. That is because the water vapor component *displaces* dry air, so that only the *total* pressure due to the partial pressures of the water vapor and dry air components must be uniform Thus we find variations in the molar column density of water vapor (see Sect. 5.3) over a typical baseline of

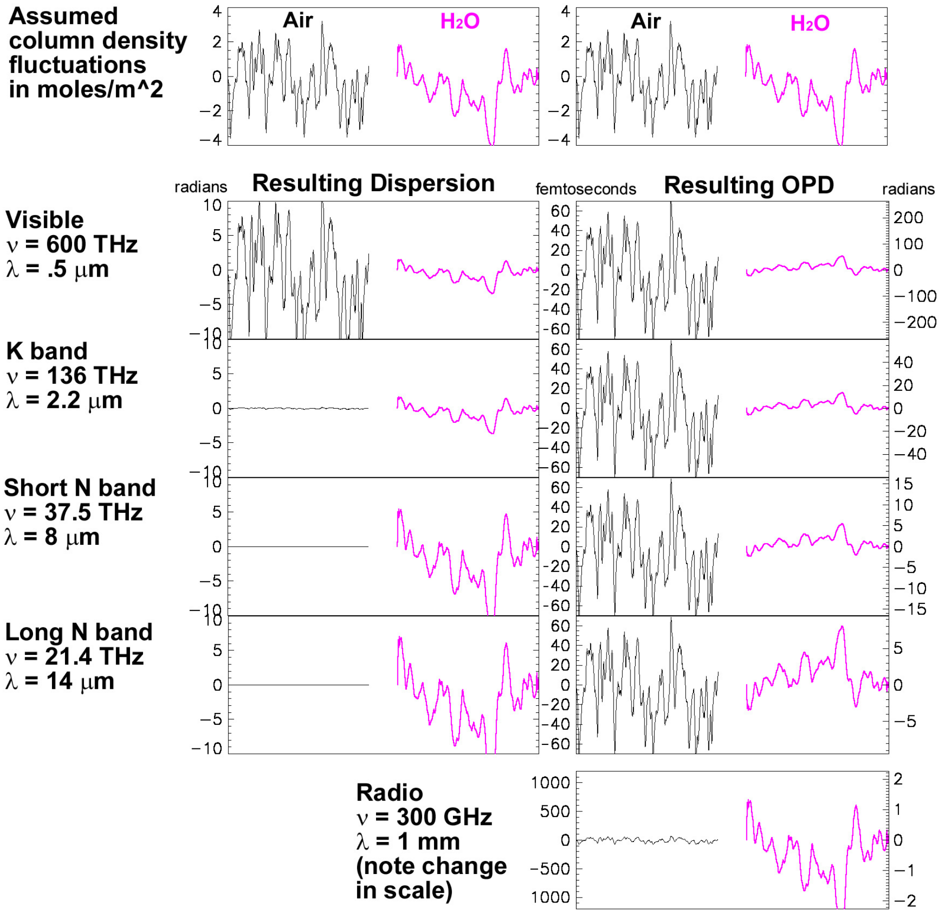

Figure 5. Atmospheric column density variations (top) of both dry air and water vapor (left and right side of each graph) are each shown at an rms level of 1.5 $mole/m^2$. Left side: dispersion given by Φ_{GD} resulting from these two components is illustrated, showing the increasing effect of water vapor dispersion at longer wavelengths. Right side: OPD ("piston") variations due to air are seen to be similar at all wavelengths, while OPD variations resulting from water vapor fluctuations have increasing relative importance at longer wavelengths, especially in the radio. Delay is labeled on the left in femtoseconds (60 fs = 18 μm vacuum path), while labels on the right side show the phase shift (in radians) associated with that delay at the specified wavelength.

similar magnitude to the 1.5 $mole/m^2$ cited above for dry air. But in this case we are talking about not 10^{-5}, but perhaps 10^{-2} of the total water vapor in the air column.

5.2. Wavelength Dependence of OPD and Dispersion Fluctuations

The net effect of these two separate random processes at different wavelengths is illustrated in Fig. 5. At the top we separately plot a fictitious density variation of dry air of rms level 1.5 $mole/m^2$, followed by a variation of WDA also at the level of 1.5 $mole/m^2$ rms, depicted as a lower-frequency fluctuation (note that these waveforms are not actual simulations of atmospheric power spectra but only included for illustrative purposes). Due to each source, the effect of the fluctuation on first order dispersion phase Φ_{GD} (left) and on OPD (right) is shown for different wavelengths.

5.2.1. OPD fluctuations

We identify OPD variations observed by a near IR (or visible) interferometer primarily with the variations in the density of dry air, which has a refractive index whose magnitude is 5 times larger than WDA. However at wavelengths longer than 7 microns (below 40 THz), the magnitude of $\hat{n}_{wda}$ increases substantially, causing it to become a significant contributor to atmospheric OPD fluctuations affecting an interferometer. This is much more true at radio wavelengths, where the effect of water vapor inhomogeneities dwarfs the effect of dry air temperature fluctuations in causing phase variations in a radio interferometer. This extreme effect is depicted at the bottom right of Fig. 5, in which the plot of OPD at millimeter wavelengths due to water vapor fluctuations requires a scale 20 times larger than the graphs above it.

5.2.2. Dispersion fluctuations

Although the effect of WDA on OPD variations is small in the near IR, it still far outweighs dry air as a source of random dispersion. The left side of Fig. 5 depicts dispersion variations due to dry air and due to humidity fluctuations. We can see that even at K band WDA will cause about 50 times as much random dispersion compared to dry air fluctuations at the same level. At N band, this discrepancy rises to 5000! So at infrared wavelengths, we can associate the *random* component of dispersion variations as being a result of humidity variations. This is no longer true at visible wavelengths where the dispersion of dry air has a larger effect, as also shown in Fig. 5. In the visible regime, random dispersion due to small fluctuations in the column density (due to thermal variations) of dry air becomes very observable, and is therefore largely correlated with OPD variations, a principle which can be exploited for wide-angle astrometry.[11]

5.3. Magnitude and Timescales of Water Vapor Fluctuations

While the fluctuation of dry air column densities due to atmospheric turbulence has been well studied and is familiar to interferometrists, comparable statistics involving water vapor inhomogeneities in the atmosphere are rare. In the past, water vapor has been most easily observed in its large effect on OPD variations in radio astronomy, and controlled observations over a 100 meter baseline using a radio beacon from a geosynchronous satellite have yielded convincing statistics.[12] A typical level of fluctuations over that baseline of 1.5 $mole/m^2$ is cited. Although water vapor is expected to obey Kolomogoroff statistics as we expect for dry air OPD fluctuations, that study indicates that the outer scale of turbulence for water vapor is *much* larger (many kilometers) leading to generally slower fluctuations, with typically about half of the spectral power (using a 100 meter baseline) below .01 Hz. It also appears that the level of water vapor inhomogeneities experiences greater night-to-night variations than we find for OPD (or seeing).

Although first order dispersion is difficult to measure with VINCI because of its relatively narrow bandwidth, it is often possible to observe the average Φ_{GD} in an observation (typically a few minutes long) as we have already seen in Fig. 4A. In some strong observations it is possible to track dispersion variations *within* the observation with some significance. One example is shown in Fig. 4B during 100 seconds of a VINCI observation of Sirius over a 16 meter baseline. The 150^o full scale of Φ_{GD} in this plot corresponds to a water vapor column density difference of about 2.2 $mole/m^2$. Note the large error bars in this graph (or any such data obtained from VINCI) preventing one from observing the structure of the fluctuations on time scales shorter than about 5 seconds. Since VINCI observations are limited to a few minutes, we are also unable to directly observe fluctuations on longer timescales than that.

A number of VINCI observations using the 16 meter baseline have indicated levels around .5 $mole/m^2$ rms, but this may be the "best case" due to selection effects which make the process difficult to observe when it is much stronger. Observation of Φ_{GD} using the 66 meter VLTI baseline have been even more difficult to interpret; one estimate gave an rms value of 1.8 $mole/m^2$. Because of the limited observation time, none of these measurements sampled frequency components slower than .01 Hz. However the residuals in the graph of Fig. 4A, for instance, puts an upper limit on low frequency components at about .25 $mole/m^2$ rms (with the 16 meter baseline). Similar analyses with 66 meter baseline observations have been unsuccessful.

6. DEGRADATION OF INTERFEROMETRIC MEASUREMENTS DUE TO DISPERSION

6.1. Dispersion Effects when Phase-Referencing from a Different Wavelength

An important observing mode using MIDI, will become available when a separate near IR fringe tracking interferometric instrument becomes available for concurrent use during MIDI observations. Either using the

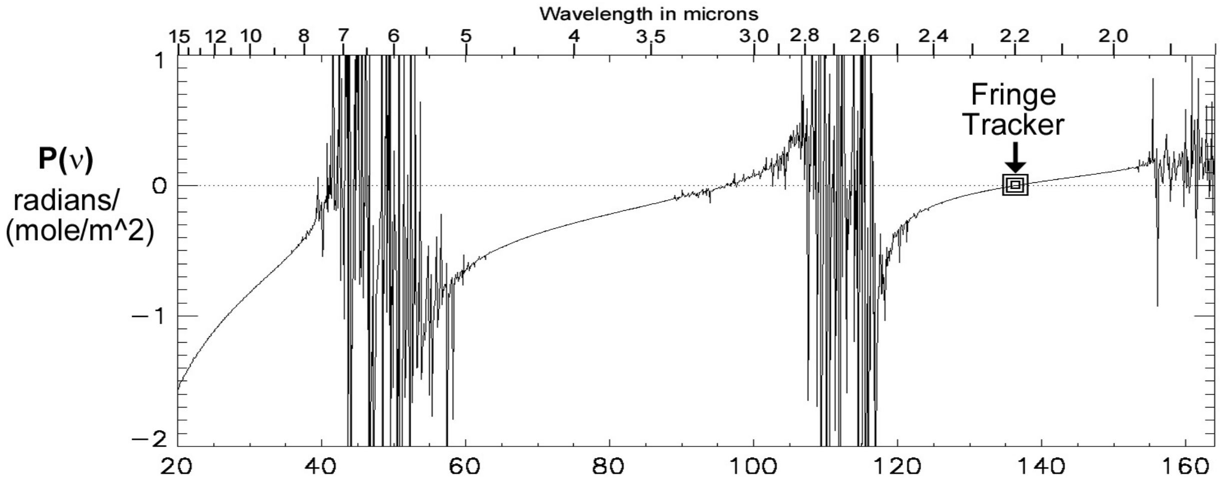

Figure 6. Coefficient for obtaining the phase referencing error ϕ at optical frequency ν due to a differential water vapor column density D, assuming fringe tracking at 136 THz.

light from the same object (FINITO) or from an off-axis reference star (PRIMA), it will become possible to conduct observations at $10\mu m$ on faint objects for which insufficient correlated flux at N band would be received in order to fringe track. A stable phase reference will permit interferometric *imaging* of arbitrary objects (whose intrinsic visibility may be very low) as is routine in radio interferometry, and also will be used for precision narrow-angle astrometry. However a major problem will arise from the effects of water vapor which will cause a displacement between the fringe position detected at the near IR tracking wavelength, and that at the wavelength at which visibility (including phase) measurements are performed.

The refractivity of dry air has only a very small variation across the spectrum, so unmodelled air densities in the delay lines and random atmospheric fluctuations will track almost identically between the target and the reference wavelength. For water vapor, however, that is not the case. Thus, for an instantaneous differential water vapor column density D_{H_2O} there will be an offset τ in the phase delay observed between the fringe tracker operating at (for instance) 136 THz ($2.2\mu m$), and MIDI observing at an optical frequency ν between 20 and 40 THz, simply given by

$$\tau = (\hat{n}_{water}(\nu) - \hat{n}_{water}(136\,THz))\, D_{H_2O} \ .$$

This will translate into a *phase* error of

$$\phi = 2\pi\nu\tau = P(\nu)\, D_{H_2O}$$

where $P(\nu)$ is the coefficient of phase referencing error per $mole/m^2$ of water vapor which is plotted in Fig. 6. Thus unmonitored water vapor in the instrumental paths can subject a visibility measurement to a systematic phase error with respect to a reference star position. Random *atmospheric* water vapor fluctuations may be too slow to effectively average to zero within an observation period, also producing a net phase error of this sort.

What's more, short-term random atmospheric water vapor variations will have an additional decoherencing effect if they are not much smaller than a radian during an integration period. The rms value of that phase error is given by P multiplied by the rms level of differential water vapor fluctuations. It can be seen that water vapor fluctuations at the level of 1.5 $mole/m^2$ would lead to rms phase fluctuations of 1.2 radians rms at 30 THz ($10\mu m$) and over 2.3 radians rms at 20 THz ($15\mu m$). 1.2 radians rms would cut the observed visibility in half, and 2.3 radians would essentially destroy it. Clearly, compensation using an external dispersion detector will be required in order for the potential of off-axis phase referencing interferometry to be realized at mid infrared wavelengths. It would also be required to prevent unacceptable errors in phase referenced imaging or astrometry at *any* wavelength which is not identical to the sensing wavelength of the fringe tracker.

6.2. Dispersion in Nulling Interferometry

Nulling is the "most coherent" technique being proposed for ground-based interferometry, and it is thus the most sensitive to dispersion errors. Much of the research in that field has been directed toward beam combination with an "achromatic" phase offset of 180°, and it can be seen in Table 1 that even small amounts of differential water vapor will have a devastating impact on the achromaticity of that phase shift. The resulting null depth, assuming the OPD is adjusted for perfect nulling at $10\mu m$, is shown in the third column of Table 1 using the full N band, and in the fifth column assuming detection of only a 20% bandwidth centered around 30 THz.

It should likewise be noted that in the case of *large* water vapor imbalances, compensation for first order dispersion alone will be insufficient to achieve deep nulls. Table 2 shows the *residual* nulling leakage experienced after removal of first order dispersion. Evidently, a hardware dispersion compensator will be required which correctly matches the *specific* dispersion curve of water vapor, or it will require more than one degree of freedom in order to allow adjustment for these higher order terms.

6.3. Dispersion effects on visibility estimation

We shall assume that dispersion is not so severe as to undermine the coherence within each detector element at the hardware level. Then the effect that dispersion has on the estimation of visibility *amplitude* depends very much on the visibility estimator in use. Any practical visibility estimator will be immune to first order dispersion. The effect of first order dispersion will then only be to introduce a false phase into the visibility determination. Constraining the phase determined at the center optical frequency ν_0, this will introduce a phase slope of $-\Phi_{GD}\,(\nu-\nu_0)/\nu_0$. We have calculated Φ_{GD} for small water vapor differential column densities between 0 and 1 $mole/m^2$, for interference in the N band. Table 1 shows Φ_{GD} (in degrees) first for interference over the full band and then for a 20% bandwidth observation around 30 THz where the average dispersion constant is a bit lower. Such a visibility phase error will occur for any static but unknown differential water vapor, or from the residual level of random water vapor fluctuations that did not average to zero during the course of a finite observation period.

Table 1

Water vapor	Full band		20% bandwidth	
$(mole/m^2)$	Φ_{GD}	Null	Φ_{GD}	Null
0.0	0.°	0.0000	0.°	0.0000
0.1	15.0°	0.00091	13.8°	0.00011
0.2	30.0°	0.00362	27.6°	0.00040
0.3	45.0°	0.00811	41.4°	0.00088
0.4	60.0°	0.0144	55.3°	0.00158
0.5	75.0°	0.0224	69.1°	0.00245
0.6	90.0°	0.0321	82.9°	0.00353
0.7	105.°	0.0436	96.7°	0.00480
0.8	120.°	0.0566	110.°	0.00626
0.9	135.°	0.0712	124.°	0.00793
1.0	150.°	0.0873	138.°	0.00977

Table 2

Water vapor	Visibility	Fringe	Null with
$(mole/m^2)$	reduction	width	1^{st} order corr.
0.	1.0000	2.50	0.00000
1.	0.9995	2.50	0.00043
2.	0.9984	2.52	0.00151
3.	0.9966	2.57	0.00338
4.	0.9939	2.65	0.00603
5.	0.9906	2.85	0.00930
6.	0.9865	3.40	0.0134
7.	0.9819	3.57	0.0180
8.	0.9765	3.72	0.0234
9.	0.9705	3.82	0.0294
10.	0.9638	3.95	0.0361

It can be seen that very tight control of dispersion would be required in order to measure first order phase functions with any precision. Paradoxically, *higher order* components of object phase can be measured with much better precision.[10]

Consider a 100 meter differential delay line path. With the typical humidity at Paranal, that would contain about 10 $mole/m^2$ excess water vapor. That will cause significant *higher order* dispersion. In Table 2 we consider the effect of large water vapor column densities on interferometry using the full N band.

It is possible to have an estimator of visibility amplitude which is immune to such a level of dispersion, such as spectrally dispersed detection with incoherent averaging, or "fourier mode" long delay scanning. In the latter case, the effect of high order dispersion will be to increase the required length of a scan in order to capture most of the fringe energy. The scan length required to capture the central 95% of the fringe energy is tabulated in Table 2 in terms of the number of wavelengths at $\nu_0 = 30$ THz ($10\mu m$).

Visibility amplitude estimators which measure the peak of the fringe *envelope* (such as "ABCD") will have a sensitivity reduction due to higher order dispersion, also given in Table 2. Of course, if the magnitude of the dispersion is *known*, then any such visibility loss can be calibrated using this model.

Realtime or off-line *fringe tracking* will naturally be affected by dispersion as an algorithm attempts to locate the OPD of a signal whose different frequency components have different delays! However large amounts of dispersion due to air in the delay lines can be predicted, leaving only first order dispersion. *Group delay tracking*, which is planned for the realtime control of MIDI, is insensitive to residual first order dispersion.[13]

7. DETECTION AND CORRECTION OF RANDOM DISPERSION FLUCTUATIONS

Just as a "fringe tracker" in a stellar interferometer is used to monitor and correct for atmospheric OPD fluctuations, one can do the same for differential water vapor fluctuations in the optical paths. This therefore involves both *estimation* of the differential water vapor column density, and *correction* for the associated amount of dispersion in order to (as well as possible) cancel its effect so as to produce an end result identical to what would have been measured if there had been no water vapor present at all.

Once again, there are two components contributing to differential water vapor column densities. The *instrumental* contribution, due to water vapor present in the air of the light paths (including delay lines) between the telescopes and the interferometric instrument, can be rather large, but is, in principle, directly measurable. On the other hand, the *atmospheric* water vapor in the light paths in the direction of the star can only be measured through one or another type of remote sensing. Either type of dispersion, if not monitored, can lead to a bias in the phase of visibility measurements. Random dispersion fluctuations, as we have seen, may also entail second-order effects which will reduce the coherence of observations and hence reduction of measured visibility amplitudes (or increase in leakage in a nulling interferometer). Let us now briefly look at options for the detection of dispersion within the interferometer's infrastructure, detection of atmospheric dispersion, and correction for those quantities.

7.1. Detection of Instrumental Dispersion

The VLTI tunnels are currently equipped with electronic thermometers and a barometer; these measurements are recorded frequently with a high accuracy. However we have seen that the main component of instrumental dispersion at longer wavelengths (and a substantial component even at NIR) is the water vapor content. Currently only the outdoor humidity is monitored using a low resolution hygrometer. Thus it is proposed that an upgraded system for monitoring the composition of the internal air paths be employed, which would, at the very least, include higher precision hygrometers at a number of tunnel locations.

A more elaborate solution would be to install a two-color laser monitoring system along the light paths in order to detect humidity variations. This would then be sensitive to the total column density of water vapor, exactly what would be needed to correct the interferometer's results, so long as it sampled substantially the same light path taken by the stellar light. The future PRIMA facility includes a laser metrology system along a path corresponding to the central obstruction in the beams from the telescopes. Simultaneous interferometric detection of light from a second laser at a properly chosen wavelength, could enable this metrology system to double as a column density hygrometer.

7.2. Tracking of Random Atmospheric Dispersion

Wideband interferometric observations at high signal-to-noise ratios, will generally enable the direct observation of dispersion fluctuations from the interferometric data itself, providing that the data is produced in a way which retains relative phase information between frequency components. However under poorer SNR's, use of the primary interferometric data will fail in this regard, and secondary estimation procedures must be sought. Let us now examine a few possibilities.

7.2.1. Water vapor radiometry

We can benefit from research conducted over the last several years in millimeter wave astronomy, for which transmission through differential water vapor column densities is the main source of atmospheric phase variations, resulting in image degradation. Thus there has been interest in monitoring these fluctuations using the thermal emission of water vapor at such wavelengths. Proposed schemes either involve measuring the total background power emitted by the atmosphere, or focus on spectral features of water vapor, such as a strong (and therefore saturated) water vapor line at 183 GHz, or an optically-thin but substantial line at 22 GHz. Such a radiometer must be carefully calibrated at regular intervals, especially inasmuch as the desired result involves subtraction of two similar quantities (each total water vapor column) in order to obtain the differential water vapor measurement. Experiments using this concept have been successful in reducing the magnitude of phase fluctuations due to atmospheric water vapor fluctuations, and systems of this sort are in the plans of future millimeter and submillimeter arrays.[14]

One possibility for 10 micron interferometry, would be for MIDI, in spectrally-dispersed operation, to monitor fluctuations in the atmospheric emission from strong water vapor lines around $7 - 7.5\mu m$. By also observing background emission at adjacent wavelengths at which water vapor is transparent, one could remove the effect of system temperature fluctuations not associated with water vapor emission. However such a scheme has a major flaw. At $7\mu m$ thermal emission is very sensitive to temperature variations in the atmosphere. For instance, emission from water vapor at 293° C would be 60% higher than it is from the water vapor at 273° C! Thus a huge error would occur due to the uncertainty of the temperature from which the fluctuations were occurring.

Desirable wavelengths for water vapor radiometry would lie at longer wavelengths, not included within the passband of MIDI, thus requiring detection by a separate instrument rather than MIDI itself. Of course that could even include millimeter wave receivers (and antennas) for the strong 183 GHz line mentioned above. However there may be more practical options for the VLTI than radiometry, given these complications.

7.2.2. Water vapor densitometry

At much shorter wavelengths, there are water vapor lines which do not emit radiation at atmospheric temperatures, but do absorb starlight. A particularly strong set of water vapor lines is found around $2.5\mu m$, at the very edge of the K band. By measuring the strength of transmitted starlight at a well defined wavelength region and comparing it to adjacent wavelengths not affected by this source of absorption, it is expected that a good sensitivity to water vapor column density could be obtained, given a sufficiently bright object.

However we will ultimately wish to observe fairly dim objects, also using rather dim phase reference stars. As we go deeper, the sensitivity of this method will deteriorate, exactly when we need it the most! Thus we would seek a more sensitive gauge of atmospheric water vapor column density.

7.2.3. Laser illuminated remote sensing

Lasers are capable of projecting powerful spatially coherent monochromatic beams, and have thereby found use in "laser guide star" technology for adaptive optics, as well as other applications involving remote sensing of the atmosphere. It is not excluded that a remote sensing scheme for water vapor in the laser's beam could be developed, and that this might overcome the sensitivity issues faced when using starlight. It could be imagined that one could measure backscatter from water molecules at a wavelength near a spectral line, or measure florescence by water excited by a powerful laser beam in the atmosphere. This could be an area for future research clearly having applications beyond astronomical interferometry.

7.2.4. K band interferometric sensing of differential water vapor

Typically the column density of water vapor in the path of starlight will be 100 $mole/m^2$ while the randomly varying component over a typical baseline will have an rms value of only 1 $mole/m^2$. One general drawback of the previous methods of determination of this varying component, is that the determination is a result of *subtracting* two large absolute determinations for the two (or more) elements of the interferometer in order to obtain the value relevant for correction of dispersive phases. Interferometric detection of the dispersion itself is a more direct way of observing the *differential* water vapor column density without facing the calibration requirements imposed by a "differencing" scheme.

What is then proposed, is direct measurement of the dispersion interferometrically, by detecting the difference in the phase delays between two wavelengths between which the refractive index of water vapor changes substantially. An object which is too faint to provide low noise interferometric detection at N band, will often have sufficient correlated flux in the near infrared to adequately observe water vapor dispersion. More importantly, using the future PRIMA facility of the VLTI, a faint object can be coherently integrated using a phase reference from a brighter off-axis object within the isoplanatic patch. The light from that *reference star* could just as well be used to monitor atmospheric water vapor fluctuations

Rather than focussing on the absorption lines around $2.5\mu m$, where the refractive index fluctuates wildly, we use the larger flux available from the continuum where the dispersion is smooth. The fringe sensor unit (FSU) of PRIMA is designed to track OPD fluctuations using light in the K band. We would propose to split the K band light into two spectral channels: 120 - 140 THz and 140 - 160 THz, detecting each separately. The phase delay between fringe trackers operating at these two wavelength bands provides a direct measure of differential dispersion, due to the slope of water vapor's refractive index in this region (see Fig. 2).

This would appear to be a feasible and sufficiently sensitive method according to the following calculation. We consider a reference star with a correlated K magnitude of 15 (about the expected limit for PRIMA). Considering the strehl ratio of the adaptive optics system, throughput through the VLTI, and detector quantum efficiency, we might hope for 5% of the flux incident on the 8 meter telescopes to be interferometrically detected at K band. Dividing that light into two wavelength channels will allow each detector to receive about 5000 photons per second from a 15th magnitude star. If the optical detectors were photon noise limited at that level, then each subsystem could measure the phase at its wavelength with an rms error of about .02 radians using the photons received in 1 second (1 second is about the required update period for a dispersion detector).

The change in the phase delay between the band centers at 130 and 150 THz, is about $\Delta\hat{n} = \hat{n}(150)-\hat{n}(130) \approx .2fs/(mole/m^2)$ of differential water vapor column density. Using that coefficient, the net .03 radian rms noise in a 1 second measurement translates to an error of about .17 $mole/m^2$ rms. This is a sufficient accuracy for phase correction even at 20 THz ($15\mu m$) where it entails a residual phase error of about .3 radians. Thus it would appear that a correctly designed two color K band reference star interferometric sensor would be sufficient to detect differential water vapor dispersion at the required level even using a fairly faint object.

While such a scheme avoids subtracting two large numbers to get a result, it does have a potential pitfall inasmuch as it involves *extrapolation* of a small phase delay in the K band to a much larger shift at long wavelengths. For instance, the .2 fs shift between the two K band wavelengths due to 1 $mole/m^2$ of differential water vapor, gets magnified to 4.5 fs at 30 THz ($10\mu m$) and 12.5 fs at 20 THz ($15\mu m$). We are thus sensitive to errors involving imperfect knowledge of the refractive index of water vapor. For instance, with a total range of 5 $mole/m^2$, a 10% error in the extrapolation coefficient would cause a 6 fs error at 20 THz, amounting to .8 radians. More troublesome, in this regard, would be sensitivity to other possible dispersive gasses at K band which would have a totally different extrapolation coefficient. But in the absence of any such complications, such an extrapolation, once calibrated and verified on a bright source, would appear feasible and sufficiently accurate to largely correct the dispersion problems we have discussed.

7.3. Dispersion Correction

Correction for the effects of dispersion can either be accomplished *in hardware*, or post-detection in the data analysis. The emphasis in this paper has been on correcting the data in the analysis stage, which is obviously simpler. Nulling interferometry is an exception; for obtaining deep nulls hardware compensation is mandatory.

One possible argument in favor of hardware compensation, is that it is *closed loop*, that is, the dispersion detector detects not the dispersion itself, but the *residual* dispersion after correction. An open loop system is dependent on the accuracy of calibration of the dispersion detector and modelling of the dispersion. However this might not be problematic.

Hardware dispersion compensation can be effected using transmission through one or more dispersive materials[1] whose effective thicknesses are modulated by shifting of wedges. An alternative hardware approach is transmission through a pressurized gas cell containing an appropriate quantity of the actual gasses for which compensation is required. A special pump could rapidly add and remove gas to follow dispersion fluctuations.

Note that a shorter gas cell could be used by increasing the maximum pressure allowed in the cell, however this would fail for water vapor when the vapor pressure of water is exceeded, causing condensation. Otherwise one would require a *heated* gas cell.

8. CONCLUSIONS

We have seen that dispersion is a serious problem affecting the coherence of wideband interferometry and needs to be further studied. Both atmospheric and instrumental dispersion can degrade interferometric results in a number of ways. As we go to longer wavelengths in the IR, water vapor plays an increasing role in dispersion. The actual refractive index of water vapor (and other dispersive gasses) needs to be better measured in order to accurately model its effects and correctly extrapolate data from dispersion monitors. Realtime tracking of these dispersive components will be required in the coming generation of phase-coherent instruments, in order to realize the potentials of phase referenced astrometry, imaging, nulling, and extrasolar planet detection.

ACKNOWLEDGMENTS

We wish to acknowledge that some data included herein is based on observations made with the European Southern Observatory telescopes obtained from the ESO/ST-ECF Science Archive Facility. We would also like to thank Richard Mathar of MPIA Heidelberg for his valuable work in modelling the dispersion of water vapor and atmospheric gasses.

REFERENCES

1. W. J. Tango, "Dispersion in stellar interferometry," *Applied Optics* **29**, pp. 516–521, Feb. 1990.
2. P. R. Lawson, "Bandwidth limitations and dispersion in optical stellar interferometry," *Applied Optics* **35**, pp. 5122–5124, Sept. 1996.
3. B. Edlen, "The refractive index of air," *Metrologia* **2**, pp. 71–80, 1966.
4. J. C. Owens, "Optical refractive index of air: dependence on pressure, temperature and composition," *Applied Optics* **6**, pp. 51–59, 1967.
5. P. E. Ciddor, "Refractive index of air: new equations for the visible and near infrared," *Applied Optics* **35**, pp. 1566–1573, 1995.
6. R. J. Mathar, "Computed dispersion of water vapor in the atmospheric window at $10\mu m$." see http://www.mpia.de/homes/mathar/public/matharHitr.ps.gz, July 2002.
7. H. Matsumoto, "The refractivities of water vapour for CO2 laser lines," *Optics Communications* **50**, pp. 356–358, July 1984.
8. R. J. Hill and R. S. Lawrence, "Refractive index of water vapor in infrared windows," *J. Opt. Soc. Am. A,* **3**, p. 66, Jan. 1986.
9. R. L. Akeson, M. R. Swain, and M. M. Colavita, "Differential phase technique with the Keck Interferometer," in *Proc. SPIE 4006, Interferometry in Optical Astronomy, Pierre J. Lena; Andreas Quirrenbach; Eds.*, pp. 321–327, July 2000.
10. J. A. Meisner, "Scientific and technical results from VINCI using coherent integration of fringe visibility," in *Astrophysics and Space Science, Proc. JENAM 2002 VLTI workshop, The Very Large Telescope Interferometer: Challenges for the Future, to be published,*
11. M. M. Colavita, M. Shao, and D. H. Staelin, "Two-color method for optical astrometry: theory and preliminary measurements with the Mark III stellar interferometer," *Applied Optics* **26**, pp. 4113–4122, Oct. 1987.
12. O. P. Lay, "The temporal power spectrum of atmospheric fluctuations due to water vapor," *Astronomy and Astrophysics Supplement Series* **122**, pp. 535–545, May 1997.
13. J. Meisner, "Fringe tracking and group delay tracking methods for MIDI," in *Proc. 36th Liege International Astrophysical Colloquium, From optical to millimetric interferometry: scientific and technological challenges, J. Surdej; J. P. Swings; D. Caro; A. Detal; Eds.*, **36**, pp. 225–231, July 2001.
14. M. C. Wiedner, R. E. Hills, J. E. Carlstrom, and O. P. Lay, "Interferometric Phase Correction Using 183 GHz Water Vapor Monitors," *Astrophysical Journal* **553**, pp. 1036–1041, June 2001.